Linear- and nonlinear-optical properties of GaN thin films

J. Miragliotta, D. K. Wickenden, T. J. Kistenmacher, and W. A. Bryden

Applied Physics Laboratory, The Johns Hopkins University, Johns Hopkins Road, Laurel, Maryland 20723-6099

Received December 7, 1992

Results of a linear- and nonlinear-optical investigation of GaN thin films epitaxially deposited onto (0001)-oriented sapphire are reported. Wavelength- and angle-dependent linear transmission measurements were used to determine the thickness and the refractive index in the 500–1200-nm spectral region for a series of six GaN films. Analysis of angle-dependent, second-harmonic (SH) transmission profiles at 532 nm provided a quantitative evaluation of $\chi^{(2)}_{xzx}$, $\chi^{(2)}_{zxx}$, and $\chi^{(2)}_{zzz}$ and a determination of the GaN lattice structure and tilt angle between the optical axis of the film and the surface normal of the sample. Dispersion effects between 500 nm and 1.064 μm prevented efficient SH production in individual GaN films that were greater than 2.5 μm in thickness. However, field calculations on a proposed multilayer GaN–sapphire structure observed a ninefold increase in the transmitted SH power as compared with a single GaN film.

1. INTRODUCTION

Gallium nitrade (GaN) is a wide-band-gap, III–V compound semiconductor that crystallizes in a hexagonal wurzite structure. During the past decade research pertaining to the growth and preparation of metal nitride thin films has culminated in the development of crystalline samples with nonconventional deposition techniques such as metal organic chemical vapor deposition (MOCVD) and magnetron sputtering.[1–4] The renewed experimental activity regarding the material characterization of this metal nitride is in part due to the direct band gap of ~3.4 eV in undoped GaN, which can be tailored for the production of tunable electro-optic devices in the UV and visible wavelength range of the spectrum when this material is alloyed with either AlN or InN. However, the development of photonic devices such as UV LED's and laser diodes has been hampered by the inability to produce GaN samples that possess the electronic properties (mobility, etc.) required for commercial application.[5,6]

During this recent development period little attention has been given to the characterization of the optical properties of GaN thin films. Unlike the electronic properties, which are degraded by crystal defects such as gain boundaries, nitrogen vacancies, and unintentionally introduced impurities, the linear-optical parameters such as the refractive index are much less sensitive to these imperfections. In addition, the noncentrosymmetric structure of the GaN crystal makes this material capable of generating a second-order nonlinear-optical response, such as second-harmonic (SH) generation, from the bulk region of the crystal. In fact the optical nonlinearity of the material provides a source for noninvasive, analytical investigations of the crystalline structure and orientation. From a technological viewpoint there are numerous nonlinear optical applications, e.g., optical communications and frequency conversion, that rely on second-order optical nonlinearities.[7–9] Despite these potentials, only a handful of nonlinear-optical investigations have been performed on GaN thin films, and little has been reported on the possible applications for all-optical devices.

In this paper we report the results of a linear- and nonlinear-optical investigation of a number of GaN thin films that were grown on the (0001) surface of a sapphire substrate in a MOCVD reactor. The transmitted SH power from the GaN–sapphire samples was found to possess a sensitivity to the quality of the crystal structure and orientation of the GaN film relative to that of the underlying sapphire substrate. The combination of linear- and nonlinear-optical transmission measurements permitted a determination of the wavelength-dependent refractive index from 500 to 1200 nm, the film thickness, and the magnitude of the nonlinear susceptibility elements for a series of six GaN films. In addition the angular dependence of the SH response permitted a determination of the misalignments between the surface normal of the sample and the optical axis of the GaN film. Analysis of the optical results showed no appreciable variation in either the refractive index or the nonlinear susceptibility tensor elements for the GaN samples ranging in thickness from 0.74 to 5.3 μm; however, there was a considerable decrease in the SH peak intensity as the film thickness was increased beyond 2.5 μm owing to the short coherence length (~3 μm) in GaN in the visible and near-IR wavelength region. Despite the phase-matching limitation in the GaN films, the magnitudes of the nonlinear coefficients were found to be at least an order of magnitude larger than those of KDP or crystalline quartz.

In Section 2 a brief review of the electromagnetic theory used to model the nonlinear-optical response of thin films is presented. This subject has received considerable attention for more than three decades,[10–12] and only those issues pertinent to this investigation are presented. A detailed section on the experimental procedure, describing the epitaxial growth technique, film characterization, and optical measurements, precedes the presentation of the optical results and discussion. A comparison of these results with earlier nonlinear investigations, both experimental and theoretical, is presented in the Results and Discussion section. Finally, a hypothetical nonlinear device composed of alternating GaN and linear dielectric films illustrates an enhancing mechanism for the SH conversion efficiency for nonlinear materials that are limited by a short coherence length.

0740-3224/93/081447-10$06.00

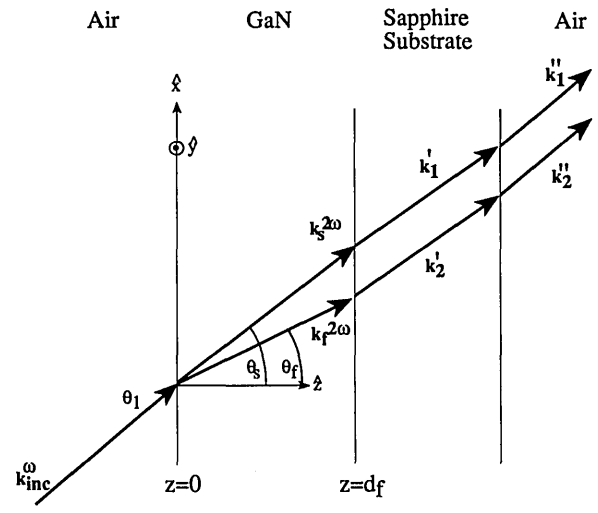

Fig. 1. Schematic of SHG in a thin GaN film on a sapphire substrate. The wave vectors of each field are discussed in the text. The refracted angle for the transmitted beams is exaggerated. Only the harmonic fields are shown in the film and sapphire substrate. The unit vectors $\hat{x}$ and $\hat{z}$ define the plane of incidence. The unit vector $\hat{y}$ points out of the page and is along the GaN surface.

2. THEORY

In previous treatments of the nonlinear electromagnetic response of a thin dielectric film at frequency 2ω to an incident light source of frequency ω, tractable solutions of Maxwell's equations for nonlinear media were deduced such that the usual boundary conditions for the fields at the plane interfaces between the nonlinear and the linear media were satisfied. These solutions were obtained by generalizing the laws of reflection and refracton to include nonlinear source terms, which were induced in the film at frequency 2ω. This procedure permitted the construction of generalized Fresnel formulas for the evaluation of the intensity and the field polarization conditions of the transmitted and the reflected harmonic beams. Detailed discussions of this nonlinear-optical problem for thin films can be found in Refs. 10, 13, and 14.

An illustration of the experimental sample under investigation is shown in Fig. 1. In this schematic a linearly polarized field at frequency ω is incident upon a GaN–air interface at angle θ_1 and is transmitted into the film at angle $\theta_2 = \theta_s$. The plane of incidence is defined as the x–z plane. We have attempted to account for optical effects that are related to the spatial quality of the experimental light source; we do so by incorporating a Gaussian beam profile into the incident beam,[11,15] i.e.,

$$E_{\mathrm{inc}}^{\omega}(x,y) = E_0 \exp\left[-(x - d_f \tan\theta_2)^2 \left(\frac{\cos\theta_1}{w_0}\right)^2\right] \exp\left[-\left(\frac{y}{w_0}\right)^2\right], \tag{1}$$

where E_0 is the magnitude of the incident field, w_0 is the radius of the Gaussian beam at the focus (waist), the x–y plane defines the surface of the GaN film, and d_f is the thickness of the film. The linear field in the film (not shown) can induce a nonlinear polarization wave that propagates with wave vector $\mathbf{k}_s(2\omega) = 2\mathbf{k}_2(\omega)$, where $\mathbf{k}_2(\omega)$ is the wave vector of the transmitted linear field. In addition to this inhomogeneous wave, a free harmonic wave is generated at the surface of the nonlinear slab with wave vector $\mathbf{k}_f(2\omega)$, as is shown in Fig. 1. The total harmonic field in the film is a superposition of these two terms. Since the direction and the magnitude of the wave vectors of these respective fields are not equal unless $n_f(\omega) = n_f(2\omega)$, the free and the driven harmonic waves will propagate with different phase velocities in the film. The phase difference leads to an interference between these fields, which manifests itself as an oscillatory behavior in the transmitted SH signal as the optical path length in the nonlinear material is varied. Thus, for efficient generation of harmonic power, the difference between the index at the fundamental and the harmonic frequencies must be negligible. This can be accomplished in materials that are negatively birefringent, such as KDP crystal, but phase matching in GaN is prohibited owing to the positive uniaxial nature of the refractive index in this material.

For the specific crystal symmetry of GaN ($6mm$) the induced nonlinear polarization in the metal nitride film has the following form in Cartesian coordinates[13,16]:

$$\begin{aligned} P_{x'}^{(2)}(2\omega) &= 2\chi_{x'z'x'}(2\omega)E_{z'}(\omega)E_{x'}(\omega), \\ P_{y'}^{(2)}(2\omega) &= 2\chi_{x'z'x'}(2\omega)E_{z'}(\omega)E_{y'}(\omega), \\ P_{z'}^{(2)}(2\omega) &= \chi_{z'x'x'}(2\omega)[E_{x'}(\omega)^2 + E_{y'}(\omega)^2] + \chi_{z'z'z'}(2\omega)E_{z'}(\omega)^2, \end{aligned} \tag{2}$$

where $\chi_{x'z'x'}$, $\chi_{z'x'x'}$, and $\chi_{z'z'z'}$ are the nonzero elements in the second-order nonlinear susceptibility tensor. For an ideal wurzite structure these elements are not independent and are geometrically related by the expressions[17]

$$\chi_{x'z'x'} = \chi_{z'x'x'}, \qquad \chi_{z'x'x'} = -\chi_{z'z'z'}/2. \tag{3}$$

The primes in the expressions for the induced nonlinear polarization denote the response viewed in the coordinate frame of the crystal (x', y', z') and not with respect to the laboratory coordinate system (optical frame in Fig. 1). For evaluation of the nonlinear response in the laboratory coordinate system, the expressions in Eqs. (2) were transformed from the crystal into the optical coordinate system by use of orthogonal matrices constructed from the Euler angles between the two respective reference frames.[18] The transformation procedure was tedious but straightforward and permitted the nonlinear polarization components in the laboratory frame to be described by the following expressions:

$$\begin{aligned} P_{x\,\mathrm{lab}}^{(2)} &= \sum_{i=x',y',z} A_{xi} P_{i\,\mathrm{xtal}}^{(2)}, \\ P_{y\,\mathrm{lab}}^{(2)} &= \sum_{i=x',y',z} A_{yi} P_{i\,\mathrm{xtal}}^{(2)}, \\ P_{z\,\mathrm{lab}}^{(2)} &= \sum_{i=x',y',z'} A_{zi} P_{i\,\mathrm{xtal}}^{(2)}, \end{aligned} \tag{4}$$

where A_{ij} are the transformation tensor elements that contained the rotational information relating the two coordinate frames (xtal stands for crystal). Note that the 2ω notation has been omitted on all harmonic polarization

and field terms. The expressions in Eqs. (4) are directly dependent on the transformation between the crystal and the laboratory reference frame, permitting information concerning the orientational relationship between the GaN thin film and the sapphire substrate to be deduced from the SH transmitted intensity.

In the present investigation x-ray analysis of the GaN films determined that the direction of the optical axis for all films (z' direction in the crystal frame) was within 3° of the surface normal of the sample (z direction in the optical or laboratory frame). Under these orientational conditions the off-diagonal elements of A_{ij} are negligible, and the diagonal terms are nearly unity. Therefore the laboratory and the crystal frames of reference are nearly coincident with one another, i.e.,

$$\begin{aligned} P^{(2)}_{x\,\mathrm{lab}} &\cong P^{(2)}_{x'\,\mathrm{xtal}}, \\ P^{(2)}_{y\,\mathrm{lab}} &\cong P^{(2)}_{y'\,\mathrm{xtal}}, \\ P^{(2)}_{z\,\mathrm{lab}} &\cong P^{(2)}_{z'\,\mathrm{xtal}}. \end{aligned} \tag{5}$$

In general an accurate determination of the thin-film orientation from the nonlinear response will require knowledge of the transformation angles between the crystal and the laboratory frames, as is demonstrated in Section 4; however, the dependence of the induced polarization in the laboratory frame can now be estimated from the expressions shown in Eqs. (2).

In this experimental investigation all measurements used optical excitation geometries, which led to the efficient generation of only p-polarized SH signals, i.e., $P^{(2)}_{y\,\mathrm{lab}} \cong 0$. For the purpose of constructing an analytical expression for the transmitted SH field, the p-polarized nonlinear polarization can be decomposed into components that are either along $[P^{(2)}_{\parallel}]$ or perpendicular to $[P^{(2)}_{\perp}]$ the direction of propagation:

$$\begin{aligned} P^{(2)}_{\parallel} &= P^{(2)}_{z}(\cos\theta_s) + P^{(2)}_{x}(\sin\theta_s), \\ P^{(2)}_{\perp} &= -P^{(2)}_{z}(\sin\theta_s) + P^{(2)}_{x}(\cos\theta_s), \end{aligned} \tag{6}$$

where θ_s is the transmitted angle of the nonlinear source field in the GaN film. The expressions in Eqs. (6) are used as the source terms in the transmitted harmonic field in the thin film.

The calculational guideline of the preceding discussion provides a procedure for determining the solutions to Maxwell's equation in a nonlinear thin film bound by linear media. Included in the model are the existence of multiple reflections for the linear and the nonlinear fields at the two GaN interfaces, since both the linear and the nonlinear transmission data in Section 4 suggest their presence. The underlying substrate is considered to have no second-order nonlinearity (as was verified experimentally). With the above-mentioned considerations, the harmonic field transmitted into the sapphire substrate (fields k_1' and k_2' in Fig. 1) is

$$E_t^{2\omega}(x,y) = \pi[A_1 g(x) + B_1 h(x)] \times \exp\left[-2\left(\frac{\cos\theta_1}{w_0}\right)^2\right]\exp\left[-\left(\frac{y}{w_0}\right)^2\right], \tag{7}$$

where

$$g(x) = \exp\left\{-2\left[\frac{d_f(\tan\theta_f)(\cos\theta_1)}{w_0}\right]^2\right\}\exp\left[\frac{4d_f x(\tan\theta_f)(\cos^2\theta_1)}{w_0^2}\right],$$

$$h(x) = \exp\left\{-2\left[\frac{d_f(\tan\theta_2)(\cos\theta_1)}{w_0}\right]^2\right\}\exp\left[\frac{4d_f x(\tan\theta_2)(\cos^2\theta_1)}{w_0^2}\right], \tag{8}$$

$$\begin{aligned} A_1 = {} & -\exp(i\phi_f)\frac{[n_t(\cos\theta_f) + n_f(\cos\theta_t)][Q_1 n_f + Q_2(\cos\theta_f)]}{(n_f\cos\theta_t)(n_t\cos\theta_f)} - \exp(-i\phi_f)\frac{[n_f(\cos\theta_t) - n_t(\cos\theta_f)][Q_2(\cos\theta_f) - Q_1 n_f]}{(n_f\cos\theta_t)(n_t\cos\theta_f)} \\ & + \left\{\frac{[n_f(\cos\theta_t) - n_t(\cos\theta_f)][Q_1 n_f + Q_2(\cos\theta_f)]\exp(i\phi_f)}{D(n_f\cos\theta_t)(n_t\cos\theta_f)} + \frac{[n_t(\cos\theta_f) + n_f(\cos\theta_t)][Q_2(\cos\theta_f) - Q_1 n_f]\exp(-i\phi_f)}{D(n_f\cos\theta_t)(n_t\cos\theta_f)}\right\} \\ & \times \{[n_r(\cos\theta_f) - n_f(\cos\theta_r)][n_f(\cos\theta_t) + n_t(\cos\theta_f)]\exp(i\phi_f) + [n_f(\cos\theta_t) - n_t(\cos\theta_f)] \\ & \times [n_r(\cos\theta_f) + n_f(\cos\theta_r)]\exp(-i\phi_f)\}, \end{aligned} \tag{9}$$

$$B_1 = \frac{2(Q_3 n_t + Q_4\cos\theta_t)}{n_t\cos\theta_t} - \frac{2[Q_4(\cos\theta_t) - Q_3 n_t]}{n_t\cos\theta_t}\left\{\frac{[n_f(\cos\theta_t) - n_r(\cos\theta_r)][n_t(\cos\theta_f) + n_f(\cos\theta_t)]\exp(i\phi_f)}{D} + \frac{[n_f(\cos\theta_t) - n_t(\cos\theta_f)][n_r(\cos\theta_f) + n_f(\cos\theta_r)]\exp(-i\phi_f)}{D}\right\}, \tag{10}$$

with

$$\begin{aligned} D = {} & [n_f(\cos\theta_t) - n_t(\cos\theta_f)][n_r(\cos\theta_f) - n_f(\cos\theta_r)] \\ & \times \exp(i\phi_f) + [n_f(\cos\theta_t) + n_t(\cos\theta_f)] \\ & \times [n_r(\cos\theta_f) + n_f(\cos\theta_r)]\exp(-i\phi_f). \end{aligned} \tag{11}$$

In these expressions the terms Q_i contain the induced nonlinear polarization in the film and are given by the expressions

$$Q_{1(3)} = \frac{(\cos\theta_s)P^{(2)}_{\perp}}{n_s^2 - n_f^2}\frac{(\sin\theta_s)P^{(2)}_{\parallel}}{n_f^2}, \tag{12}$$

where the subscript 1(3) indicates that $P^{(2)}_{\parallel}$ and $P^{(2)}_{\perp}$ in the expression were evaluated at $z = 0(d_f)$, and

$$Q_{2(4)} = \frac{n_s P^{(2)}_{\perp}}{n_s^2 - n_f^2}, \tag{13}$$

where the subscript 2(4) indicates that $P^{(2)}_{\perp}$ in this expression is evaluated at $z = 0(d_f)$. The index n_s denotes the refractive index of the nonlinear source term and is equal

to $n_f(\omega)$. In these expressions the refractive indices labeled n_r, n_f, and n_t are evaluated at 2ω. On the refractive-index, cosine, and sine terms the subscripts 1, f, t, r, respectively, refer to the incident, the film, the transmitted, and the reflected media. The terms ϕ_f represents the phase of the free harmonic wave as it propagates from the front to the back of the film, i.e.,

$$\phi_f = 2n_f \omega d_f(\cos\theta_f)/c, \tag{14}$$

where ω is the fundamental frequency and c is the speed of light in vacuum. Since the source terms propagate with a phase velocity that is proportional to the index of the film at ω, the expressions in Eqs. (7)–(11) demonstrate that multiplication of the Q_i and ϕ_f terms will lead to an interference profile in the transmitted SH signal owing to the phase mismatch.

The harmonic field that is transmitted across the sapphire–air interface (k_1'' and k_2'' in Fig. 1) contains a Fresnel factor that takes into account the effects of linear reflection and refraction at this linear interface. In determining the transmitted SHG power across the sample interface, we have integrated the harmonic intensity of this beam,

$$I^{2\omega} \propto (E_t^{2\omega})^*(E_t^{2\omega}), \tag{15}$$

over the sapphire–air interface and normalized this quantity to the power and the beam area of the incident excitation source. The expression for the normalized SH power is given by

$$P^{2\omega} = F_1\Bigg(A_1^*A_1 + B_1^*B + (A_1^*B + B_1^*A_1) \times \exp\left\{-\frac{(d_f\cos\theta_1)^2[(\tan\theta_2) - (\tan\theta_f)]^2}{w_0^2}\right\}\Bigg), \tag{16}$$

where F_1 is the Fresnel factor that accounts for transmission of the SH intensity across the sapphire–air interface:

$$F_1 = \left[\frac{2n_t\cos\theta_t}{n_t(\cos\theta_1) + n_1(\cos\theta_t)}\right]^2. \tag{17}$$

In the expression for SH transmitted power, the asterisk denotes the complex conjugate of that quantity. The exponential term in Eq. (16) describes the effects that arise when a Gaussian is used rather than a plane-wave spatial profile. This correction factor also accounts for the dispersion differences in the free and the bound waves and the finite size of the beam diameter. For the samples examined in this investigation the thicknesses of the GaN films were such that $d_f \ll w_0$ and $\theta_2(\omega) \sim \theta_f(2\omega)$. Therefore the exponential function is ~1 and has no significant effect on the generation of a SH signal in these samples.

An examination of Eq. (7)–(11) shows that the film parameters required for numerical analysis of SH transmission data include the refractive index of the material at ω and 2ω, the film thickness d_f, the Euler angles that relate the crystal and the optical reference frames, and the nonvanishing nonlinear coefficients. Although the algebraic expression in Eq. (16) is rather cumbersome, it represents a tractable solution to the nonlinear response of a thin film. In practice one can extract the nonlinear coefficients from the experimental second-harmonic generation (SHG) data by first determining the film's thickness and refractive index from linear transmission or reflection studies.

3. EXPERIMENTAL PROCEDURE

A primary limitation in the technological development of bulk GaN is the difficulty of obtaining crystalline material at reasonable temperatures and pressures. To overcome this problem, techniques such as MOCVD have been developed for the preparation of heteroepitaxial films, which are usually deposited on the (0001) surface of sapphire. The GaN films used in this study were grown in an Emcore vertical spinning-disk MOCVD reactor operating at a base pressure of 70 Torr. Source materials for film growth were trimethyl gallium and ammonia (NH_3), which were transported to the reactor in a nitrogen carrier gas.[1] Before film growth, x-ray diffraction results showed that the surface normal of the sapphire substrates were oriented to within 3° of the (0001) direction. The chemically polished substrates were cleaned in hot HNO_3:H_2O_2:H_2O and HCl:H_2O_2:H_2O solutions. This preparation procedure has been found to ensure epitaxial growth of GaN on (0001) sapphire.

Before initiation of continuous film growth, we predeposited a GaN nucleation layer onto the substrate by heating the sample to 600 °C and exposing it to the source materials for 50 s. Inclusion of this layer resulted in a significant improvement in the surface morphology of the subsequent growth layer, which was deposited at a substrate temperature of 1100 °C. We achieved the variation in film thickness by varying the sample's time of exposure to the source materials, which typically yielded a 1–2-μm/h growth rate. After growth the epitaxial relationship and duality of the films were verified by additional x-ray diffraction measurements. The single-crystal films were oriented with the (0001) plane of the film parallel to the (0001) plane of the substrate and a 30° azimuthal rotation of the GaN layer with respect to the underlying sapphire substrate, i.e., the $(10\bar{1}0)$ plane of the film was parallel to the $(11\bar{2}0)$ plane of the substrate.

We performed a series of linear-optical transmission measurements to determine the refractive index and film thickness of the GaN films. Normal-incidence linear transmission in the spectral range of 500–1200 nm was measured with a Perkin-Elmer 330 UV/visible spectrometer. In addition, angle-dependent linear transmission curves at 514.5 nm for light polarized parallel (p polarized) and perpendicular (s polarized) to the plane of incidence were generated for each GaN–sapphire sample by use of a Spectra-Physics 164AC Ar^+ laser as the incident light source.

We performed SHG measurements by measuring the transmitted SH signal from a GaN–sapphire sample as a function of the incident angle and the field polarization of the fundamental and the SH beam. This procedure is identical to the Maker-fringe transmission technique.[11,19] In this technique the intensity envelope and generated fringes in the SHG transmission profile provide an accurate means for determining the magnitude of the nonvanishing elements in the nonlinear susceptibility tensor and the orientation of the optical axis of the film. Q-switched radiation from a Nd:YAG pulsed laser at 1.064 μm was

used as the optical source for the SH experiments (Continuum NY82-10, ~7-ns pulse width, 10-Hz repetition rate, and single-longitudinal-mode operation). Before incidence the beam was passed through a silica plate beam splitter for the purpose of creating a reference beam for the SHG sample measurements. The sample beam was spectrally filtered to remove residual 532-nm light and was focused to a 1-mm spot (Gaussian profile) on the GaN surface with an energy density of 10 mJ/cm^2. A half-wave plate was placed in the incident beam for the purpose of selecting either *s*- or *p*-polarized incident radiation. The transmitted light from the sample was filtered to remove 1.064-μm light with appropriate color filters, analyzed with a linear polarizer, and detected with an EMI 9789QB photomultiplier tube. We verified the harmonic nature of the sample signal by demonstrating its quadratic dependence on the incident 1.064-μm intensity. The reference IR beam was transmitted through a KDP crystal whose nonlinearity generated a SH signal that was easily detected with a Scientech photodiode. The current outputs of the photomultiplier tube and photodiode were analyzed with separate gated integrators, and all data storage and analysis was performed with a Macintosh IIfx computer. We removed fluctuations in the sample signal arising from intensity variations in the incident beam by normalizing this signal to the SH signal generated in the KDP reference. Following the SHG measurements on each GaN sample, the angular dependence of the SH signal from a quartz reference crystal was determined. The nonlinear coefficient of this material has been characterized from earlier SHG studies[20] and provides an accurate means for determining the absolute magnitude of the nonlinear coefficients of the GaN film.

Sample rotation for all angle-dependent measurements was accomplished with a computer-interfaced stepping motor. Data collection was synchronized to the sample rotation and was processed by the computer interface every 0.5° as the sample was rotated ±75° about an axis along the sample surface (*y* axis in Fig. 1). For the pulsed laser studies each data point represents a 10-pulse average. Numerical analysis of the linear and the SH transmission measurements was accomplished with a least-squares nonlinear curve-fitting routine.

4. RESULTS AND DISCUSSION

A. Linear Transmission

The data in Fig. 2 show the results of the angle- and the wavelength-dependent linear transmission profiles for one of the GaN–sapphire samples. In Fig. 2(a) the *p*-polarized angular transmission results were recorded with incident *p*-polarized light at a wavelength of 514.5 nm and an incident beam size of ~1 mm. A similar transmission curve (not shown) was generated for an *s*-polarized light source at this same wavelength. Note that the rapid variation in the transmission profile in the vicinity of normal incidence was a result of multiple-beam interference in the sapphire substrate.

Shown in Fig. 2(b) is the normal-incidence transmission spectrum, which was recorded from the same GaN–sapphire sample in the 500–1200-nm spectral range. The light source for the measurements was unpolarized and collimated to a 1-mm spot size on the GaN–sapphire sample. The amplitude of the fringes in both the spectrum- and the angle-dependent transmission curves denoted the good optical quality of both the GaN thin film and the sapphire surfaces.

As is noted in Section 2, an accurate determination of the film's thickness and refractive index at 1.064 μm and 532 nm was required for a proper evaluation of the nonlinear-optical properties of the GaN films. In the present investigations the optical axis for all GaN films was directed approximately along the surface normal of the sample. For this crystal orientation the index of refraction for the extraordinary wave is given by

$$n(\theta_{\text{film}}) \cong n_o\left\{1 + (\sin^2\theta_1)\left[\frac{n_e - n_o}{(n_e n_o)^2}\right]\right\}^{1/2}, \tag{18}$$

where θ_1 is the angle of incidence at the air–GaN film interface and n_o and n_e are the ordinary and extraordinary index values, respectively. In previous optical investigations the difference between these two values was found to be ~0.02, i.e., $n_e = n_o + 0.02$.[21] Using this value as an upper limit on the birefringence in the GaN film, we calculate that there is a 0.003 increase in the index of the extraordinary beam over that of the ordinary index at the angle-of-incidence limits used in this experiment. This level of index variation has only a minimal effect on the SH power produced in the films, which permits GaN to be characterized by an angle-independent refractive index (n_o).

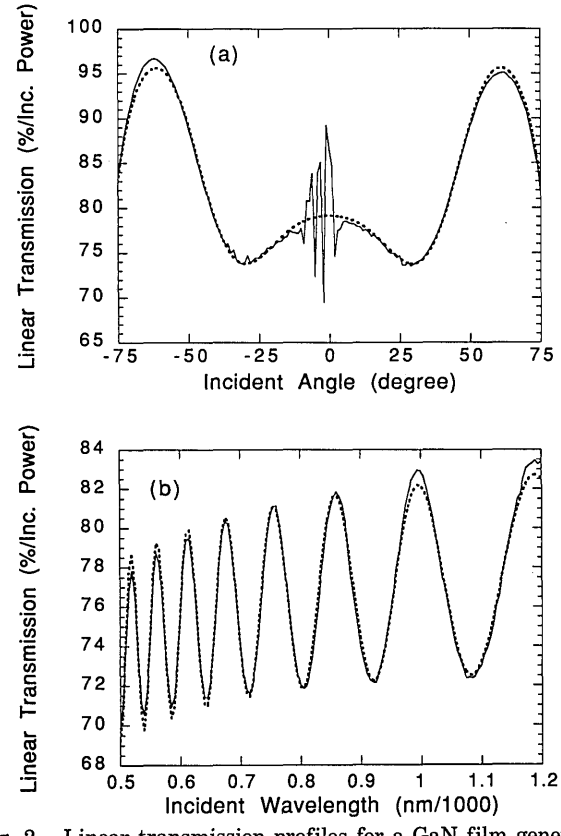

Fig. 2. Linear transmission profiles for a GaN film generated (a) by using *p*-polarized incident radiation at 514.5 nm and varying the incident angle and (b) by using unpolarized radiation at normal incidence from 500 to 1200 nm. The solid curves are the experimental data, and the dashed curves are fitted by using a classical approach in determining the transmitted intensity.

Table 1. Film Thickness and Curve-Fitting Parameters Used in the Cauchy Dispersion Formula for Determining the Refractive Index of the GaN Films

Film	Thickness (μm)	Parameter A	Parameter B
1	0.74	2.271	0.032
2	1.09	2.267	0.033
3	1.30	2.264	0.034
4	2.25	2.303	0.034
5	3.00	2.289	0.039
6	5.31	2.268	0.034

A classical electromagnetic treatment was used in modeling the linear response of the thin film in both the angle- and the wavelength-dependent linear transmission curves.[22] In the analysis the thickness of each film was evaluated from the s- and the p-polarized angle-dependent linear transmission data. With this value substituted into the electromagnetic equations for the transmitted optical power from the thin film, the normal-incidence transmission scan was similarly analyzed to yield the wavelength-dependent refractive index. In both calculations previously published results were used for the wavelength-dependent refractive index of the sapphire substrate.[23] With regard to the refractive index of the GaN samples, the transparent nature of the films (minimal absorption) in this spectral range permits this parameter to be described by the well-known Cauchy dispersion formula[22]

$$n_f = A + (B/\lambda_{inc}^2), \tag{19}$$

where the results for parameters A and B as well as the thicknesses for the six films are listed in Table 1. In the series of films investigated in this paper the index of refraction was determined to be 2.29 ± 0.02 at 1.064 μm and 2.40 ± 0.02 at 532 nm, which is consistent with the results for GaN thin films previously reported in Ref. 21. Examples of the excellent curve-fitting results for the angular and wavelength linear transmission data are included with the experimental data in Fig. 2 (dashed curves).

B. Second-Harmonic Generation

Figure 3 shows a comparison between the angle-dependent p-polarized SH light from the 1.09-μm GaN film when p-polarized [Fig. 3(a)] and s-polarized [Fig. 3(b)] incident laser sources were used for generation. The scans were performed with the same rotational assembly used in the linear experiments, permitting $\pm 75°$ angular rotations of the sample. In both angular scans the SH profile displayed a minimum at normal incidence. The position of the minimum was consistent with the expressional form for the transmitted field in Eqs. (7)–(11), which shows that this quantity is dependent on $\sin \theta_s$ only if the optical axis is aligned with the surface normal. A comparison of the two scans in Fig. 3 shows that there is an approximately 1-order-of-magnitude difference in the peak SH intensities for these respective excitation geometries. The observed SH intensity in these measurements was due entirely to the GaN film and not to the underlying sapphire substrate, as was confirmed by examining a bare (0001) sapphire sample. It was also observed that the s-polarized SH transmitted signal for these two incident excitation geometries was at least 2 orders of magnitude weaker than that of the p-polarized results. This verified our earlier assumption that the nonlinear polarization induced perpendicular to the plane of incidence, $P_y^{(2)}$, was much smaller than either that of $P_x^{(2)}$ or $P_z^{(2)}$ (parallel to the plane of incidence) when the crystal orientation had the optical axis parallel to the surface normal of the sample. A similar peak intensity ratio for the respective excitation geometries was observed for all six samples studied.

To determine the magnitude of the three nonlinear susceptibility elements in GaN, a reasonable evaluation of the experimental data was required. Examination of Eqs. (2)–(4) and relation (5) shows that a p-polarized nonlinear response to an s-polarized input field (E_y) can occur only when the incident beam couples with $\chi^{(2)}_{z'x'x'}$ in the expression for $P_z^{(2)}$. The SH scan in Fig. 3(b) is an illustration of this type of nonlinear coupling and permits an evaluation of this nonlinear coefficient without involving contributions from either $\chi^{(2)}_{x'z'x'}$ or $\chi^{(2)}_{z'z'z'}$. These data were fitted to the SH power expression in Eq. (16) with a least-squares fitting routine, and a determination of the $\chi^{(2)}_{z'x'x'}$ coefficient was obtained. The remaining two nonlinear coefficients, $\chi^{(2)}_{x'z'x'}$ and $\chi^{(2)}_{z'z'z'}$, were determined by a similar curve-fitting analysis on the SH data in Fig. 3(a). Before this procedure the crystal structure of the GaN sample was assumed to be an ideal wurzite phase, which allowed the nonlinear coefficient relations in Eqs. (3) to be used in the data analysis. Accurate fits were obtained for SH data generated with either a p-polarized or an s-polarized incident beam, as is shown by the dashed curves in Fig. 3. An identical analysis was performed on the angle-dependent SH profiles from the other five GaN films. For a number of the films it was possible to improve the fitting results by

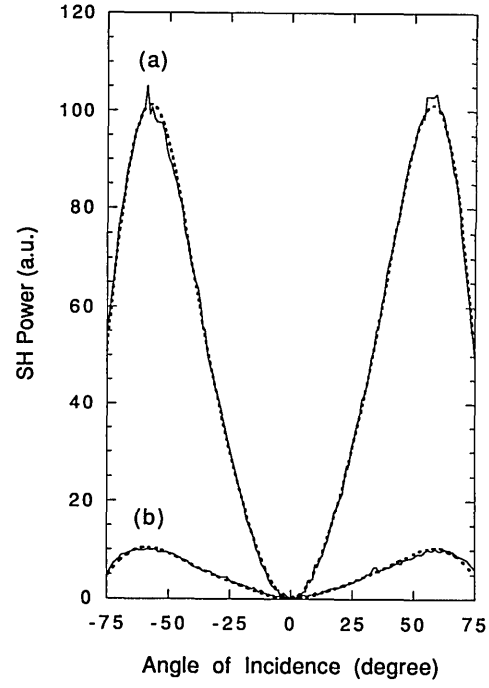

Fig. 3. Comparison of p-polarized SH signals at 532 nm from a 1.09-μm GaN film generated by using (a) p-polarized and (b) s-polarized incident light at 1.064 μm. The solid curves are the experimental data, and the dashed curves were generated by fitting to Eq. (16).

Table 2. Nonlinear Coefficients (Normalized to $\chi_{x'x'x'}$ in Quartz), Coherence Lengths, and Tilt Angles for the GaN Films

Film	$\chi_{x'z'z'}$	$\chi_{z'x'x'}$	$\chi_{z'z'z'}$	l_c (μm)	θ (deg)
1	11.03	10.56	−22.06	3.10	−3.41
2	11.33	11.33	−22.66	3.04	0.00
3	11.69	11.33	−23.38	2.92	−2.70
4	10.40	10.84	−20.82	2.94	3.97
5	11.20	11.03	−22.40	2.58	3.47
6	11.99	12.01	−23.98	2.95	3.64

choosing $\chi^{(2)}_{z'x'x'}$ to be independent of $\chi^{(2)}_{x'z'x'}$ and $\chi^{(2)}_{z'z'z'}$ but keeping the relation between $\chi^{(2)}_{x'z'x'}$ and $\chi^{(2)}_{z'z'z'}$ intact. The first assumption allowed for the possibility of structural perturbations in the crystal that led to a distortion in the ideal wurzite structure. With regard to the second criterion, we observed that the contribution from the $\chi^{(2)}_{z'z'z'}$ term in Eqs. (3) was considerably weaker than that of $\chi^{(2)}_{x'z'x'}$. This was due to the coupling dependence of $\chi^{(2)}_{z'z'z'}$ on the z component of the transmitted field in the film, which had a maximum value of only $\sim 0.4E_{\text{film}}(\omega)$ for the range of incident angles used in this experimental investigation. Although the nonlinear response from $\chi^{(2)}_{z'z'z'}$ was not negligible, the weaker contribution to the overall SH signal led to unrealistic variations (~50%) in the parameter during the SH curve-fitting analysis of a number of GaN films. A list of the nonlinear coefficients for the six GaN films is shown in Table 2. The magnitudes of these terms are normalized to the $\chi^{(2)}_{x'x'x'}$ susceptibility element in crystalline quartz. For all films the nonlinearities were at least 1 order of magnitude greater than the nonlinear coefficient in quartz. There was very little variation (<5%) in the nonlinear coefficients in the six films; the relationship between these terms was close to that for the ideal wurzite structure.

During the nonlinear-optical examination of the films the profiles of the SH signals from a number of GaN samples were found to display an asymmetry as the 1.064-μm beam was rotated through the range of incident angles. An illustration of this angular asymmetry is shown in Figs. 4(a) and 4(b), which compare the SH transmission profiles from two GaN films of thicknesses 1.09 and 1.30 μm, respectively. In both scans p-polarized incident light was used to generate a p-polarized SH response. The peak intensity in the two SH transmission profiles indicates that the magnitudes of the nonlinearity for these respective films were comparable; however, an asymmetric profile was observed for the 1.30-μm film. The asymmetry was always accompanied by a SH signal minimum at a measured angle away from normal incidence. We believe that this feature arose from a slight misorientation of the optical axis of the film with respect to the surface normal of the sample (tilt angle). As was mentioned above, x-ray diffraction measurements of the substrates and GaN films were able to determine that the optical axis for a number of the sapphire substrates and GaN films were slightly misaligned (~3°) with respect to the surface normal of the samples. The angles between the optical axis of the film and the surface normal of the sample slightly perturbs the direction of the induced polarization, since the off-diagonal elements in the transformation matrices of Eqs. (2)–(4) are no longer zero. The curve-fitting analysis of the data has determined the transformation elements A_{ij} of Eq. (4) and consequently the tilt angle for each of the GaN films. An example of the analysis is shown by the SH data in Fig. 4 (dashed curves), which compares a sample with a ~2.7° tilt [Fig. 4(a)] with a sample with no misalignment [Fig. 4(b)]. The tilt angle deduced for all GaN films is listed in Table 2.

A limitation on efficient SH production in GaN films is their rather short coherence length. Figure 5 shows the results of an examination of the angle-dependent SHG response from three GaN films of thicknesses 0.74, 2.25, and 5.31 μm, respectively. For all three scans the incident polarization of the 1.064-μm beam was p polarized. The most notable feature in this series of nonlinear responses was the dramatic decrease in the SH peak intensity as the film thickness progressed beyond the ~2.5-μm range. The reason for the decrease was mentioned in Section 2 and involves the interference of the free and the bound harmonic waves on propagation in the nonlinear film. The decrease in the SH peak intensity as the film thickness went beyond the ~2.5-μm distance was the result of the large difference in the refractive index at ω and 2ω, which manifested itself as a short coherence length in the film[11]:

$$l_c = \frac{\lambda_{\text{inc}}}{4|n_{2\omega} - n_{\omega}|}, \tag{20}$$

where l_c is the coherence length, n_ω and $n_{2\omega}$ are the indices of refraction at the fundamental and the harmonic wave-

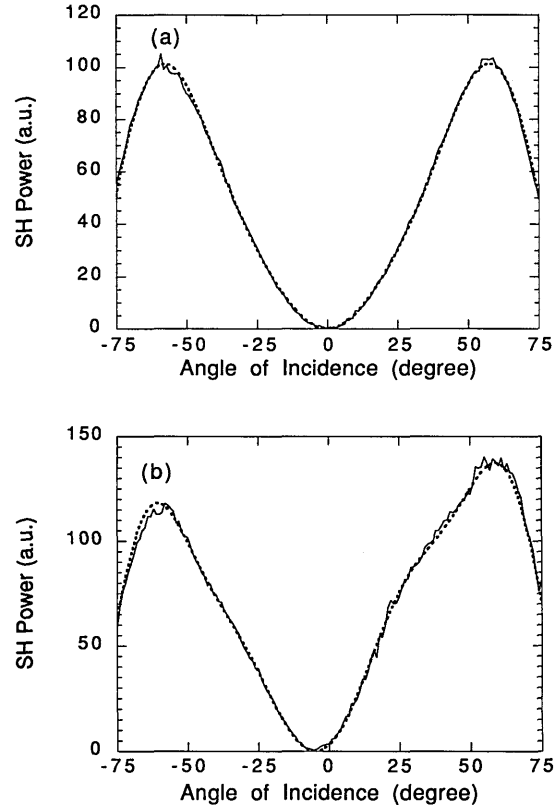

Fig. 4. Comparison of p-polarized SH signals at 532 nm, generated with p-polarized incident radiation at 1.064 μm for (a) 1.09-μm and (b) 1.30-μm films. The solid curves are the experimental data, and the dashed curves are the curve fitting analysis from Eq. (16).

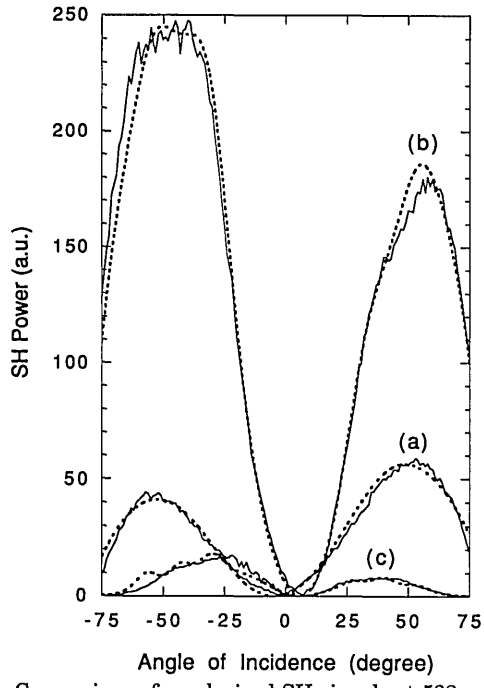

Fig. 5. Comparison of p-polarized SH signals at 532 nm, generated with p-polarized incident radiation at 1.064 μm for (a) 0.74-, (b) 2.25-, and (c) 5.31-μm GaN films. The solid curves are the experimental data, and the dashed curves are the curve fitting analysis from Eq. (16).

lengths, respectively, and λ_{inc} is the incident wavelength. This parameter has a significant effect on harmonic generation in the GaN films, as is illustrated in the SH transmission curves for the 2.25- and 5.31-μm films. For both films analysis of the SH data obtained nonlinear coefficients of approximately the same magnitude (Table 2). However, the interference between the free and the bound harmonic waves in the thicker film led to a significantly reduced SH signal versus that of the thinner film. Table 2 lists the normal-incidence optical coherence length for each film. Note that all films have a coherence length that is in the range 2.5–3 μm.

As is mentioned in the Introduction, nonlinear-optical investigations of GaN thin films are not extensive. A theoretical approach that was developed in the early 1970's relates the nonlinearity of the crystal to the degree of excess charge in the bonding region of a covalent bond.[17,24,25] The approach lends itself to a quantitative, if somewhat approximate, analysis for III–V semiconductor compounds and has been successfully applied to a number of wurzite and zinc-blende materials. In the model the bond charge tends to be highly mobile and thus highly polarizable. The linear polarizability of the bond arises from the motion of the bond charge, which is influenced by the degree of electronegativity (heteropolar) and the difference in atomic radii of the bonded atoms (homopolar). The nonlinear polarizability results from the field-induced changes in the linear susceptibility, which is dependent on the spatial displacement of the bond charge by the applied optical field. As derived by Levine,[17] the field-induced displacement depends on the average energy gap between the bonding and antibonding levels in the two-atom bond, which is simply the sum of the individual energy gaps related to the homopolar and heteropolar contributions of the bond (in this case between Ga and N). The nonlinear polarizability is derived by differentiating the linear polarizability with respect to the component of the applied field along the bond axis. An attractive feature of the bond-charge model is the *a priori* determination of the critical parameters of the nonlinear polarizability. These parameters are determined entirely from the linear response, i.e., susceptibility, and thus no adjustable parameters are required for a solution of $\chi^{(2)}$. In determination of the nonlinear susceptibility, the crystal is treated as being constructed out of the identical, cylindrically symmetric bonds, where bond–bond interactions in the solid are neglected. The nonlinear susceptibility is obtained by summing all individual polarizabilities induced on the bonds between the various atoms in the lattice. In Levine's calculations for GaN an estimate of these parameters permitted a determination of the heteropolar and homopolar nonlinearities, which were 52×10^{-9} and -115×10^{-9} esu, respectively, giving a total of -63×10^{-9} esu for d_{33}, which is equivalent to $\chi^{(2)}_{z'z'z'}/2$. This value was estimated to be approximately -50 times the calculated and experimental value of quartz[20] (1.2×10^{-9} esu). Levine mentioned that the GaN nonlinearity was an approximate value because of the lack of good refractive-index values for GaN. We believe that the ratio of approximately -22 between $\chi^{(2)}_{z'z'z'}$ in GaN and $\chi^{(2)}_{x'x'x'}$ in quartz observed in the present investigation is within the limits of the earlier theoretical calculations. In addition to the magnitude of the nonlinearities, the good fit to the experimental data achieved by using the geometric relationships in Eq. (3) for the three nonlinear coefficients indicated that the tetrahedral structure of the unit cell was largely undistorted in the GaN structure.

Comparison with previous experimental studies of epitaxial GaN films showed that the magnitude of the nonlinearities in this investigation were approximately four times smaller than that observed from earlier SH measurements.[26,27] In these earlier reports no attempt was made to determine the refractive indices of the films before the nonlinear examination and analysis. The linear properties of the GaN film were chosen *a priori* from earlier optical studies and used in the field calculations, which determined the nonlinear coefficients. In our investigation the expression for the SH power in Eqs. (16) was found to be extremely sensitive to the difference in the refractive index at the fundamental and the harmonic frequencies. Thus an *a priori* determination of these parameters could lead to a significant error in the eventual determination of the nonlinear coefficients. We believe that our approach in evaluating the linear properties before the nonlinear analysis provided a more accurate determination of the nonlinear coefficients.

It is possible to enhance the SH efficiency in GaN films by creating multilayer structures that are composed of alternating layers of GaN and a transparent linear dielectric material. A theoretical examination of harmonic generation from multilayer nonlinear structures was examined by Bethune for both isotropic[28] and anisotropic[29] (GaN) materials. The alternating nonlinear–linear structure differs from these earlier treatments in that the linear dielectric layer provides a phase shift between the transmitted fundamental and SH fields as they propagate between the nonlinear layers. The phase shift allows the SH field

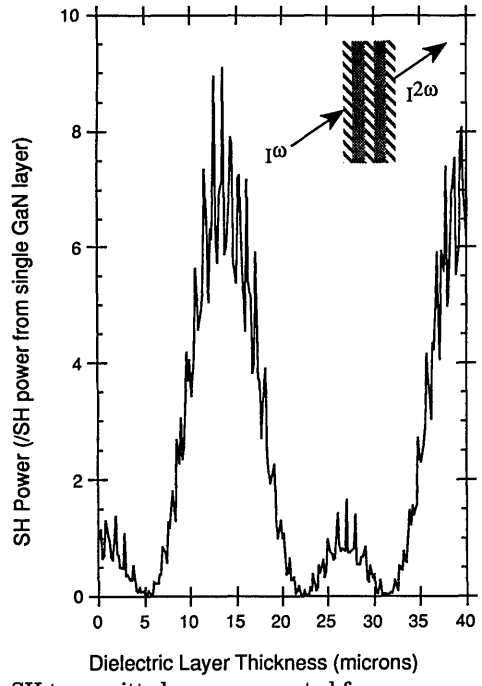

Fig. 6. SH transmitted power generated from a proposed multilayer film structure, which is shown in the inset. In the device the hatched regions are 2.2-μm GaN films (nonlinear) and the shaded regions are sapphire films (linear). The plot shows the SH transmitted power (normalized to the SH power from a single 2.2-μm GaN film) as a function of the sapphire film thickness. The fringes superimposed upon the profile are due to multiple-beam interference in the device.

from one film to mix coherently with harmonic fields that are generated in the subsequent nonlinear films, thereby eliminating the conversion-efficiency problems associated with the short coherence length in a single GaN layer. An example of a proposed multilayer structure is shown in the inset of Fig. 6. The device is composed of alternating GaN and sapphire films. Sapphire was chosen as the dielectric layer because of its transparency in the 500–1200-nm spectral region. The thickness for each GaN film was 2.2 μm, which was close to an optimum value for generating a SH response in one film when the fundamental wavelength was 1.064 μm. To achieve the correct phase-matching conditions in the device, we varied the thickness of the sapphire layer in this proposed structure until a maximum in the SH transmitted power was obtained. The graph in Fig. 6 shows the SH power from this structure (normalized to the SH power from a single 2.2-μm GaN film) as the film thickness of the two sapphire layers was varied from 0 to 40 μm. The incident angle was chosen to be 45°, since this was observed to be the optimum angle for SH generation in a single GaN film. As is shown in the plot, the transmitted harmonic power was an oscillatory function of the thickness of the dielectric layer. The SH power for this structure reached a maximum enhancement factor of ~9 over that of a single nonlinear film when the sapphire layer thickness was 13.5 μm. Experimentally we demonstrated a crude example of this film-stacking technique by placing two GaN–sapphire samples in series in a *p*-polarized 1.064-μm beam. Both GaN films were ~2 μm in thickness. The relative placement and incident angle of the two samples were chosen to optimize the SH signal from the pair of films. With this configuration we observed a SH signal from the pair, which was a factor of ~3.2 larger than the SH signal of each individual film. This example was by no means an ideal stacking situation, but it illustrated the potential for using GaN as a frequency-doubling material.

5. SUMMARY

We have used linear- and nonlinear-optical transmission measurements to determine the refractive indices and nonlinear coefficients for a series of GaN films. The SH transmission dependence on incident angle and film thickness permitted a determination of the film orientation and the coherence length. The magnitudes of the nonlinear coefficients $\chi^{(2)}_{x'z'x'}$ and $\chi^{(2)}_{z'x'x'}$ were found to be a factor of ~11 greater for the $\chi^{(2)}_{x'x'x'}$ coefficient of quartz, while the coefficient $\chi^{(2)}_{z'z'z'}$ was estimated to be different by a factor of −22. These magnitudes were consistent with an earlier bond-charge calculation of the nonlinear susceptibility elements for GaN. In addition, the accurate curve fits to the experimental data from the expressions in Eqs. (3) demonstrate the wurzite structure of the GaN lattice. Finally, we have proposed a nonlinear device constructed of alternating GaN and sapphire films. Computer simulations for the SH power obtained an enhancement factor of ~9 at 532 nm over the SH signal generated from a single GaN film and may sensibly permit the efficient use of GaN thin films as frequency-doubling elements.

Correspondence should be sent to J. Miragliotta.

REFERENCES

1. D. K. Wickenden, T. J. Kistenmacher, W. A. Bryden, J. S. Morgan, and A. Estes-Wickenden, "The effect of self-nucleation layers on the MOCVD growth of GaN on sapphire," Mater. Res. Soc. Symp. Proc. **221,** 167 (1991).
2. M. A. Khan, J. M. Van Hove, J. N. Kuznia, and D. T. Olsen, "Reflective filters based on single crystal GaN/$Al_xGaN_{1-x}N$ multilayers deposited using low pressure MOCVD," Appl. Phys. Lett. **59,** 2408 (1991).
3. J. S. Morgan, W. A. Bryden, T. J. Kistenmacher, S. A. Ecelberger, and T. O. Poehler, "Single-phase aluminum nitride films by dc-magnetron sputtering," J. Mater. Res. **5,** 2677 (1990).
4. T. J. Kistenmacher, W. A. Bryden, J. S. Morgan, and T. O. Poehler, "Characterization of rf-sputtered InN films and AlN/InN bilayers on (0001) sapphire by the x-ray precession method," J. Appl. Phys. **68,** 1541 (1990).
5. S. Strite and H. Morkoc, "GaN, AlN, and InN: a review," J. Vac. Sci. Tech. B **10,** 1238 (1992).
6. S. Nakamura, N. Iwasa, M. Senoh, and T. Mukai, "Hole compensation of *p*-type GaN films," Jpn. J. Appl. Phys. **31,** 107 (1992).
7. Y. Li, G. Eichmann, X. Luo, P. P. Ho, and R. R. Alfano, "Noncollinear SHG-based ultrafast optical signal processing for optical digital computing," Opt. Commun. **64,** 322 (1987).
8. D. R. Ulrich, "Overview: nonlinear optical organics and devices," in *Organic Materials for Nonlinear Materials,* R. A. Hann and D. Bloor, eds. (Royal Society of Chemistry, London, 1989), p. 241.
9. G. I. Stegeman, "Nonlinear guided waves," in *Contemporary Nonlinear Optics,* G. P. Agrawal and R. W. Boyd, eds. (Academic, San Diego, 1992), p. 1.
10. N. Bloembergen and P. S. Pershan, "Light waves at the boundary of nonlinear media," Phys. Rev. **128,** 606 (1962).
11. J. Jerphagnon and S. K. Durtz, "Maker fringes: a detailed comparison of theory and experiment for isotropic and uniaxial crystals," J. Appl. Phys. **41,** 1667 (1970).

12. Y. Hase, K. Kumata, S. S. Kano, M. Ohashi, T. Kondo, R. Ito, and Y. Shiraki, "New method for determining the nonlinear optical coefficients of thin films," Appl. Phys. Lett. **61,** 145 (1992).
13. Y. R. Shen, *Principles of Nonlinear Optics*, 1st ed. (Wiley, New York, 1984), Chap. 2.
14. N. Bloembergen, *Nonlinear Optics* (Benjamin-Cummings, New York, 1965), Chap. 4.
15. G. D. Boyd, H. Kasper, and J. H. McFee, "Linear and nonlinear optical properties of $AgGaS_2$, $CuGaS_2$, and $CuInS_2$, and theory of the wedge technique for the measurement of nonlinear coefficients," IEEE J. Quantum Electron. **QE-7,** 563 (1971).
16. R. Boyd, *Nonlinear Optics* (Academic, San Diego, Calif., 1992), Chap. 1.
17. B. F. Levine, "Bond-charge calculation of nonlinear optical susceptibilities for various crystal structures," Phys. Rev. B **7,** 2600 (1973).
18. H. Goldstein, *Classical Mechanics*, 2nd ed. (Addison-Wesley, Reading, Mass., 1981), Chap. 4.
19. P. D. Maker, R. W. Terhune, M. Nisenoff, and C. M. Savage, "Effects of dispersion and focusing on the production of optical harmonics," Phys. Rev. Lett. **8,** 21 (1962).
20. M. Choy and R. L. Byer, "Accurate second-order measurements of visible and infrared nonlinear of crystals," Phys. Rev. B **14,** 1693 (1976).
21. E. Ejder, Phys. Status Solidi A **6,** 442 (1971).
22. M. Born and E. Wolf, *Principles of Optics*, 6th ed. (Pergamon, New York, 1980).
23. I. H. Malitson, "Refraction and dispersion of synthetic sapphire," J. Opt. Soc. Am. **52,** 1377 (1962).
24. B. F. Levine, "A new contribution to the nonlinear optical susceptibility arising from unequal atomic radii," Phys. Rev. Lett. **25,** 440 (1970).
25. B. F. Levine, "*d*-Electron effects on bond susceptibilities and ionicities," Phys. Rev. B **7,** 2591 (1973).
26. I. M. Catalano, A. Cingolani, M. Lugara, and A. Minafra, "Nonlinear optical properties of GaN," Opt. Commun. **23,** 419 (1977).
27. T. Ishidate, K. Inoue, and M. Aoki, "SHG of epitaxially-grown GaN crystal," Jpn. J. Appl. Phys. **19,** 1641 (1980).
28. D. S. Bethune, "Optical harmonic generation and mixing in multilayer media: analysis using optical matrix techniques," J. Opt. Soc. Am. B **6,** 910 (1989).
29. D. S. Bethune, "Optical harmonic generation and mixing in multilayer media: extension of optical transfer matrix approach to include anisotropic materials," J. Opt. Soc. Am. B **8,** 367 (1991).